

# Evidence of Contribution of Intervening Clouds to GRB's X-ray Column Density

J. Wang<sup>1</sup>

wj@bao.ac.cn

## ABSTRACT

The origin of excess of X-ray column density with respect to optical extinction in Gamma-ray bursts (GRBs) is still a puzzle. A proposed explanation of the excess is the photoelectric absorption due to the intervening clouds along a GRB's line-of-sight. We here test this scenario by using the intervening Mg II absorption as a tracer of the neutral hydrogen column density of the intervening clouds. We identify a connection between large X-ray column density (and large column density ratio of  $\log(N_{\text{H,X}}/N_{\text{HI}}) \sim 0.5$ ) and large neutral hydrogen column density probed by the Mg II doublet ratio (DR). In addition, GRBs with large X-ray column density (and large ratio of  $\log(N_{\text{H,X}}/N_{\text{HI}}) > 0$ ) tend to have multiple saturated intervening absorbers with  $\text{DR} < 1.2$ . These results therefore indicate an additional contribution of the intervening system to the observed X-ray column density in some GRBs, although the contribution of the host galaxy alone cannot be excluded based on this study.

*Subject headings:* gamma-ray burst: general — intergalactic medium — methods: statistical

## 1. Introduction

Gamma-ray bursts (GRBs) are the most powerful explosions that occur throughout the universe from local to extremely high redshift (e.g., Salvaterra et al. 2009; Tanvir et al. 2009). The majority of GRBs show a long-duration ( $T_{90} > 2\text{s}$ ) and soft-spectrum in their prompt phase. It is now generally accepted that these GRBs originate from the death of

---

<sup>1</sup>National Astronomical Observatories, Chinese Academy of Sciences

young massive stars ( $\geq 25M_{\odot}$ ) according to the core-collapse model (e.g., see reviews in Hjorth & Bloom 2011 and Woosley & Bloom 2006, and references therein). The jet ignited in the core-collapse is believed to impact and shock the surrounding medium, which produces the GRB’s afterglow through synchrotron radiation at a wide wavelength range from radio to X-ray (e.g., Meszaros & Rees 1997; Sari et al. 1998).

Both X-ray and optical/near-infrared observations of afterglows provide an opportunity to study the metal abundance and column density in GRB’s local environment (e.g., Savaglio et al. 2003; Butler et al. 2003; Prochaska et al. 2007). Combining the spectral analysis in both bands suggests that the measured optical extinction is typically smaller than the expectation inferred from the X-ray-derived column density of gas by 1-2 orders of magnitude, although the column density is comparable to that in Galactic molecular clouds (e.g., Galama & Wijers 2001; Stratta et al. 2004; Schady et al. 2007, 2010; Savaglio & Fall 2004; Greiner et al. 2011; Zafar et al. 2011; Kruhler et al. 2011; Campana et al. 2006; 2010; Watson et al. 2007).

The large column density-to-dust ratio could be explained by the destruction of small dust grains out to a radius of  $\sim 10\text{pc}$  by the intense prompt emission of the GRB (e.g. Fruchter et al. 2001; Perna & Lazzati 2001; Perna et al. 2003). Campana et al. (2010) and Watson et al. (2007) claimed that the large ratio could be alternatively caused by either higher metallicity or stronger photoionization of hydrogen due to the GRB’s high energy emission. Schady et al. (2010), however, found a tight anti-correlation between the column density-to-dust ratio and metallicity, which is in conflict with the expectation inferred from the metallicity scenario. Kruhler et al. (2010) argued that the observed large ratio is mainly caused by two independent absorbers. One is a neutral absorber related to host galaxy that is located at a distance of  $10^{2-3}\text{pc}$  from the burst; the other is an ionized one that is in the vicinity of the burst.

Thanks to the *Swift* mission (Gehrels et al. 2004) and prompt follow-up observations in the optical band, a large GRB sample has recently shown that there is a correlation between the intrinsic X-ray column density and redshift (e.g., Campana et al. 2010; Behar et al. 2011; Starling et al. 2013). In addition, Campana et al. (2012) and Watson & Jakobsson (2012) show that the bursts with high column density can occur at low-to-moderate redshift when highly extinguished events are included. There is, however, a lack of bursts with low X-ray column density at high redshift. The correlation motivates various authors to argue that the X-ray column density excess could be explained by the photo-electric absorption due to diffuse intergalactic medium (IGM) or intervening absorbing clouds, even though the intrinsic absorption from a host galaxy is required for nearby GRBs (e.g., Behar et al. 2011; Starling et al. 2013; Campana et al. 2012). On the contrary, Watson & Jakobsson (2012)

argued that the intervening clouds alone seem to be insufficient to account for the large column density found in high- $z$  GRBs.

In this paper, we present a piece of evidence supporting the conclusion that the observed X-ray column density excess is at least partially caused by the cumulative effect that results from the intervening systems in the line-of-sight of a GRB. Because of the poor spectral resolution of current X-ray observations, the foreground absorption of Mg II  $\lambda\lambda 2796, 2803$  doublet is used as a tracer of the intervening systems. The paper is organized as follows. The sample selection is described in §2. §3 then compares the intervening Mg II absorption with the intrinsic X-ray column density to reveal the contribution from the intervening absorption systems.

## 2. Mg II Absorption Sample

Thanks to the rapid-response spectroscopy of high- $z$  GRB’s optical afterglows, the absorption of Mg II  $\lambda\lambda 2796, 2803$  doublet is a commonly used transition in studying the intervening absorbing clouds in the line-of-sight of a GRB, both because of the relative high abundance of Mg and because of the high strength of the transition (e.g., Prochter et al. 2006; Prochaska et al 2007; Tejos et al. 2009; Vergani et al. 2009; Cucchiara et al. 2012).

We compile a sample of all available *Swift* GRBs with intervening Mg II doublet absorption reported in literature. No cut on the intervening Mg II  $\lambda 2796$  equivalent width (EW) is used in our sample compilation. We further require that the measured rest-frame EWs of both lines in the Mg II doublet are available for each intervening absorber. The sample finally contains 29 GRBs, and is tabulated in Table 1, along with the references. All the errors reported in the table correspond to the  $1\sigma$  significance level after taking into account the proper error propagation.

For each GRB, Columns (1) and (2) list the GRB identification and measured redshift of the GRB, respectively. The redshifts of the identified intervening Mg II absorption systems are tabulated in Column (3). Columns (4) and (5) present the EW of Mg II  $\lambda 2796$  and the corresponding Mg II doublet ratio  $DR = EW(2796)/EW(2803)$ , respectively. For each afterglow with multiple intervening Mg II absorption systems, Columns (4) and (5) list the values of the intervening absorber with the lowest DR value. The corresponding redshift of the absorber is marked in boldface type in Column (3). In these afterglows, we further check if there are multiple intervening absorbers with  $DR < 1.2$  in each line-of-sight, and mark the corresponding redshifts with an asterisk in Column (3). The intrinsic X-ray column density  $N_{H,X}$  is listed in Column (6) for each of the GRBs. The column density is obtained from

the X-ray energy spectrum in the *Swift* XRT Photon Counting (PC) mode<sup>1</sup>. The spectrum taken in the Windowed Timing mode, if any, is not adopted to avoid the possible spectral evolution at early time (e.g., Campana et al. 2007; Gendre et al. 2007).

In the current sample, the X-ray column density  $N_{\text{H,X}}$  ranges from  $10^{21}$  to  $10^{22.5}$   $\text{cm}^{-2}$ . The sample reproduces the previously reported  $N_{\text{H,X}}$  versus  $z$  correlation (see the citations in INTRODUCTION). The relationship is presented in Figure 1 for the current sample. By excluding the GRBs with upper limits of  $N_{\text{H,X}}$ , a statistical test returns a Kendall’s  $\tau = 0.409$ ,  $Z$ -value of 2.81 and  $P = 0.005$ , where  $P$  is the probability that there is no correlation between the two variables. A few of GRBs with high column density and heavy optical extinction have been identified in the low-to-moderate redshift range (Campana et al. 2012; Watson & Jakobsson 2012). The heavy extinction most likely results in a selection bias against these bursts in the current sample. Watson & Jakobsson (2012) stated that the redshifts of these bursts are mainly obtained from the observations of their host galaxies.

Figure 2 shows the relation between  $N_{\text{H,X}}$  and optical extinction  $A_V$  for the current sample, when the values of  $A_V$  are reported in literature. We list the values of  $A_V$  in column (8) in Table 1. The dashed line shown in the figure marks the typical dust-to-gas ratio for the Local Group in the case with solar metallicity (Welty et al. 2012). One can see from the figure an evident excess of  $N_{\text{H,X}}$  with respect to the optical extinction, and a marginal increase of  $N_{\text{H,X}}$  with  $A_V$ . The mean value of  $N_{\text{H,X}}/A_V$  ratio is  $\approx 1.7 \times 10^{22}$   $\text{cm}^{-2}$   $\text{mag}^{-1}$ , which is highly consistent with the one reported in Covino et al. (2013).

### 3. Results and Discussions

#### 3.1. MgII doublet absorption

We use the intervening Mg II doublet absorption as a tracer of the foreground absorption system to study the origin of the X-ray column density excess detected in GRBs. The Mg II absorption traces a wide range of neutral hydrogen column density  $N_{\text{HI}}$  from  $10^{16}$  to  $10^{22}$   $\text{cm}^{-2}$  (corresponding to an EW(2796) from 0.02 to 10 Å, e.g., Churchill et al. 2000; Rao & Turnshek 2000; Rigby et al. 2002). By using the expanded SDSS/HST sample of low- $z$  Lyman- $\alpha$  absorbers, Menard & Chelouche (2009) reveals a relationship between mean  $N_{\text{HI}}$  and EW(2796), although the relationship has very large scatter.

---

<sup>1</sup>The data and spectral analysis results can be found in the UK Swift Science Data Center repository at [http://www.swift.ac.uk/xrt\\_spectra](http://www.swift.ac.uk/xrt_spectra) (Evans et al. 2009).

It has been frequently pointed out that the EW of Mg II  $\lambda$ 2976 line is a better indicator of number of individual components and/or the velocity spread of the gas than an indicator of  $N_{\text{HI}}$  (e.g., Petitjean & Bergeron 1990; Prochter et al. 2006; Gupta et al. 2009). It is noted that a low Mg II DR close to 1 more directly reflects high column density than does EW(2796) (e.g., Gupta et al. 2009 and references therein). The DR of the Mg II doublet theoretically ranges from 1.0 for completely saturated lines to 2.0 for unsaturated lines according to atomic physics. In the current sample,  $\sim 80\%$  GRBs have Mg II DRs within the range  $1 < \text{DR} < 2$  (within the errors). After taking into account the errors, the remaining GRBs listed in our sample have Mg II DRs very close to the upper and lower theoretical limits. The mean and median values of DR are 1.18 and 1.15, respectively, which means there is a strong saturation for these intervening Mg II absorption clouds.

If the X-ray column density excess was only attributed to the gas related to the host galaxy, the strength of intervening Mg II absorption is expected to be physically unrelated with the X-ray column density. Figure 3 presents the Mg II DR versus  $N_{\text{H,X}}$  diagram. A moderately strong anti-correlation can be identified from the diagram: the larger the Mg II DR, the smaller the X-ray column density will be. A statistical test yields a Kendall's  $\tau = -0.2586$  and a  $Z$ -value of 2.091 at a significance level with a probability of null correlation of  $P = 0.0365$ . These coefficients are calculated through the survival analysis to take account of the entries in which only upper limits of  $N_{\text{H,X}}$  can be obtained from observations. The anti-correlation suggests a positive relationship between the observed X-ray column density and the column density traced by the intervening Mg II absorptions. The afterglows with multiple intervening absorbers are shown by the blue points, and the afterglows with a single absorber by the red ones. The size of the blue points is scaled to the number of saturated Mg II absorbers with  $\text{DR} < 1.2$ . It seems that, as expected, the line-of-sight with more saturated absorbers tends to correspond to higher X-ray column density.

A Monte-Carlo simulation with 1,000 random experiments is performed to investigate the effect caused by the larger errors in both DR and  $N_{\text{H,X}}$ . A random sample is established by assuming a Gaussian distribution for each measurement (except for the upper limits). The Kendall's  $\tau$  test is then carried out for each of the 1,000 random samples. Again, the tests are based on the survival analysis. Figure 4 shows the distribution of the simulated Kendall's  $\tau$ . The distribution can be well described by a Gaussian function with a peak at  $\tau = -0.23$  and a standard deviation of 0.06. A weighted sum of the calculated probability of each random sample yields a total probability of null correlation of 0.368, which indicates that the significance of the correlation degrades to the  $1\sigma$  significance level when the large errors are taken into account.

### 3.2. $N_{\text{HI}}$ from $\text{Ly}\alpha$ observations

Covino et al. (2013) recently compared the X-ray column density with the neutral hydrogen column density measured from the local Lyman- $\alpha$  absorption. The comparison shows that there is a relation between the two independent measurements for some events listed in their sample. Some outliers, however, can be clearly identified from their comparison. Furthermore, the authors claimed that the relation is improved when the contribution of the intervening system is removed from the observed X-ray column density. The contribution is empirically estimated from the intervening absorption model proposed in Campana et al. (2012).

In order to additionally test the effect caused by the intervening system, the Mg II DR is plotted in Figure 5 as a function of the ratio between the column density measured from the X-ray spectrum and that measured from the local Lyman- $\alpha$  absorption. The host galaxy hydrogen column density ( $N_{\text{HI}}$ ) obtained from the Lyman- $\alpha$  observation is listed in Column (7) in Table 1 for each GRB. The data are mainly taken from Fynbo et al. (2009), except for GRB 100219 (Thone et al. 2013). GRB 060607 and GRB 050908 are not shown in the plot because of their extremely large ratios. The estimated ratios are  $\log(N_{\text{H,X}}/N_{\text{HI}}) = 4.85 \pm 0.19$  and  $< 3.9$  for GRB 060607 and GRB 050908, respectively. The corresponding Mg II DRs are as small as  $1.02 \pm 0.08$  and  $1.32 \pm 0.03$ . One can see from the figure that the GRBs with large  $N_{\text{H,X}}/N_{\text{HI}}$  ratio (i.e.,  $\log(N_{\text{H,X}}/N_{\text{HI}}) > 0.5$ ) tend to have heavy line saturation with Mg II DR close to 1. Since a small Mg II DR caused by the saturation of Mg II  $\lambda 2976$  line reflects a high neutral hydrogen column density, the trend suggests that the large X-ray column density observed in some GRBs could be attributed to an additional absorption caused by their intervening system. Similar to Figure 3, the line-of-sights with multiple (single) saturated absorbers are presented by the blue (red) points. The size of the blue point is again scaled to the number of saturated absorbers. Although there is only one saturated absorbers in the line-of-sight of GRB 060607, the GRBs with  $\log(N_{\text{H,X}}/N_{\text{HI}}) > 0$  tend to be associated with more than one saturated absorber.

### 3.3. Conclusions and Discussions

The discrepancy between  $N_{\text{HI}}$  obtained from optical data and that from X-ray spectral analysis has been frequently reported in previous studies (e.g., Starling et al. 2007; Schady et al. 2010). By using the Mg II doublet absorption that is taken from afterglow optical spectroscopy as a tracer of neutral hydrogen column density, the statistical study in this paper reveals a connection in which a GRB with high X-ray column density tends to be associated with large intervening neutral hydrogen column density. This connection therefore

indicates an additional contribution of the intervening system to the observed  $N_{\text{H,X}}$  in some GRBs on observational grounds, which, however, does not mean a firm exclusion that the high  $N_{\text{H,X}}$  values can be due to the host galaxy component alone. The contribution to X-ray column density needs to be quantified for each component to properly explain observations, which is a hard task at present because the current X-ray spectral resolution is too low to identify individual absorption features.

The revealed connection between intervening hydrogen column density and  $N_{\text{H,X}}$  can naturally explain the observed correlation between  $N_{\text{H,X}}$  and redshift by including an extra X-ray absorption contributed by the intervening system. The scenario in which  $N_{\text{H,X}}$  is dominantly contributed by the intervening system has been proposed by many previous studies. By doubling the number of intervening clouds that are derived from QSO studies, the simulation done by Campana et al. (2012) suggests that the intervening absorber scenario is a plausible explanation for the X-ray column density excess. With a more realistic model, Starling et al. (2013) proposed that the absorption due to the cumulative effect of intervening Lyman- $\alpha$  clouds can equally explain the X-ray column density excess. An alternative possible explanation of the discrepancy is the photoelectric absorption due to diffuse cold or warm intergalactic medium (Behar et al. 2011; Starling et al. 2013). A further support for the contribution of the intervening systems may come from the fact that the relation between  $N_{\text{H,X}}$  and  $N_{\text{HI}}$  become tighter after subtracting to the X-ray values the mean contribution from intervening systems (see Covino et al. 2013). Under some conditions, the intervening absorbers can also affect the  $A_{\text{V}}$  determination and possibly contribute to the observed  $N_{\text{H,X}}$  versus  $A_{\text{V}}$  correlation found by Watson et al. (2013) and Covino et al. (2013).

Watson & Jakobsson (2012) argued that the intervening clouds seem to be insufficient to explain the column density excess after taking into account of the metallicity evolution and unjustified overabundance of intervening clouds in the GRB’s line-of-sight. In fact, a much weaker overabundance was recently revealed in Cucchiara et al. (2012) by re-analyzing a large sample of intervening Mg II absorption. Watson et al. (2013) recently proposed that the absorption by Helium in the host H II region is responsible for most of the observed X-ray column density, after excluding other scenarios. Their argument is based on the  $N_{\text{H,X}} - A_{\text{V}} (N_{\text{HI}})$  correlation and a change of  $N_{\text{H,X}}/A_{\text{V}}$  ratio with redshift that is similar to cosmic metallicity evolution. A recent study shows that the evolution of  $N_{\text{H,X}}/A_{\text{V}}$  is likely caused by the lack of bursts with small  $N_{\text{H,X}}$  at high redshift rather than the evolution of  $A_{\text{V}}$ , although the physical origin of the lack has not been determined at the current stage (Covino et al. 2013). This result seems to be inconsistent with the implication of the scenario proposed in Watson et al. (2013).

The author thanks an anonymous referee for his/her careful review and helpful sugges-

tions for improving the manuscript. The author thanks James Wicker for help with language. The study is supported by the National Basic Research Program of China (grant 2009CB824800) and by the National Natural Science Foundation of China under grant 11003022. We gratefully acknowledge funding for *Swift* at the University of Leicester from the UK Space Agency. This work uses data provided by the UK *Swift* Science Data Center at the University.

## REFERENCES

- Behar, E., Dado, S., Dar, A., & Laor, A. 2011, *ApJ*, 734, 26
- Butler, N. R., Marshall, H. L., Ricker, G. R., Vanderspek, R. K., Ford, P. G., Crew, G. B., Lamb, D. Q., & Jernigan, J. G. 2003, *ApJ*, 597, 1010
- Campana, S., et al. 2006, *A&A*, 449, 61
- Campana, S., et al. 2007, *ApJ*, 654, 17
- Campana, S., Thone, C. C., de Ugarte Postigo, A., Tagliaferri, G., Moretti, A., & Covino, S. 2010, *MNRAS*, 402, 2429
- Campana, S., Salvaterra, R., Melandri, A., Vergani, S. D., Covino, S., D’Avanzo, P., Fugazza, D., Ghisellini, G., et al. 2012, *MNRAS*, 421, 1697
- Covino, S., et al. 2013, *astro-ph/arXiv:1303.4743*
- Cucchiara, A., et al. 2012, *astro-ph/arXiv:1211.6528*
- Churchill, C. W., Mellon, R. R., Charlton, J. C., Jannuzi, B. T., Kirhakos, S., Steidel, C. C., & Schneider, D. P. 2000, *ApJ*, 543, 577
- de Ugarte Posigo, A., et al. 2010, *A&A*, 513, 42
- Evans, P. A., et al. 2009, *MNRAS*, 397, 1177
- Fynbo, J. P. U., et al. 2009, *ApJS*, 185, 526
- Fruchter, A., Krolik, J. H., & Rhoads, J. E. 2001, *ApJ*, 563, 597
- Galama, T. J., & Wijers, R. A. M. J. 2001, *ApJ*, 549, 209
- Gendre, B., Galli, A., Corsi, A., Klotz, A., Piro, L., Stratta, G., Boer, M., & Damerджи, Y. 2007, *A&A*, 462, 565

- Greiner, J., et al. 2011, *A&A*, 526, 30
- Gehrels, N., et al. 2004, *ApJ*, 611, 1005
- Gupta, N., Srianand, R., Petitjean, P., Noterdaeme, P., & Saikia, D. J. 2009, *MNRAS*, 398, 201
- Hjorth, J., & Bloom, J. S. 2011, *astrp-ph/arXiv:1104.2274*
- Kruhler, T., et al. 2011, *A&A*, 543, 108
- Menard, B., & Chelouche, D. 2009, *MNRAS*, 393, 808
- Meszáros, P., & Rees, M. J. 1997, *ApJ*, 482, 29
- Perna, R., & Lazzati, D. 2001, *ApJ*, 580, 261
- Perna, R., Lazzati, D., & Fiore, F. 2003, *ApJ*, 585, 775
- Petitjean, P., & Bergeron, J. 1990, *A&A*, 231, 309
- Prochaska, J. X., et al. 2007, *ApJS*, 168, 231
- Prochter, G. E., et al. 2006, *ApJ*, 648, 93
- Rao, S. M., & Turnshek, D. A. 2000, *ApJS*, 130, 1
- Rigby, J. R., Charlton, J. C., & Churchill, C. W. 2002, *ApJ*, 565, 743
- Salvaterra, R., Della Valle, M., Campana, S., Chincarini, G., Covino, S., D’Avanzo, P., Fernandez-Soto, A., Guidorzi, C., et al. 2009, *Nature*, 461, 1258
- Sari, R. Piran, T., & Narayan, R. 1998, *ApJ*, 497, 17
- Savaglio, S., & Fall, S. M. 2004, *ApJ*, 614, 293
- Savaglio, S. Fall, S. M., & Fiore, F. 2003, *ApJ*, 585, 638
- Schady, P., et al. 2007, *MNRAS*, 377, 273
- Schady, P., et al. 2010, *MNRAS*, 401, 2773
- Starling, R. L. C., Willingale, R., Tanvir, N. R., Scott, A. E., Wiersema, K., O’Brien, P. T., Levan, A. J., & Stewart, G. C. 2013, *astro-ph/arXiv:1303.0844*

- Starling, R. L. C., Wijers, R. A. M. J., Wiersema, K., Rol, E., Curran, P. A., Kouveliotou, C., van der Horst, A. J., & Heemskerk, M. H. M. 2007, *ApJ*, 661, 787
- Stratta, G., Fiore, F., Antonelli, L. A., Piro, L., & De Pasquale, M. 2004, *ApJ*, 608, 846
- Tanvir, N. R., Fox, D. B., Levan, A. J., Berger, E., Wiersema, K., Fynbo, J. P. U., Cucchiara, A., & Krühler, T., et al. 2009, *Nature*, 461, 1254
- Tejos, N., Lopez, S., Prochaska, J. X., Bloom, J. S., Chen, H. W., Dessauges-Zavadsky, M., & Maureira, M. J. 2009, *ApJ*, 706, 1309
- Thone, C. C., et al. 2013, *MNRAS*, 428, 3590
- Vergani, S. D., Petitjean, P., Ledoux, C., Vreeswijk, P., Smette, A., & Meurs, E. J. A. 2009, *A&A*, 503, 771
- Watson, D., Hjorth, J., Fynbo, J. P. U., Jakobsson, P., Foley, S., Sollerman, J., & Wijers, R. A. M. J. 2007, *ApJ*, 660, 101
- Watson, D., & Jakobsson, P. 2012, *ApJ*, 754, 89
- Watson, D., et al. 2013, *ApJ*, 768, 23
- Welty, D. E., Xue, R., & Wong, T. 2012, *ApJ*, 745, 173
- Woosley, S. E., & Bloom, J. S. 2006, *ARA&A*, 44, 507
- Zafar, T., Watson, D., Fynbo, J. P. U., Malesani, D., Jakobsson, P., & de Ugarte Postigo, A. 2011, *A&A*, 532, 143



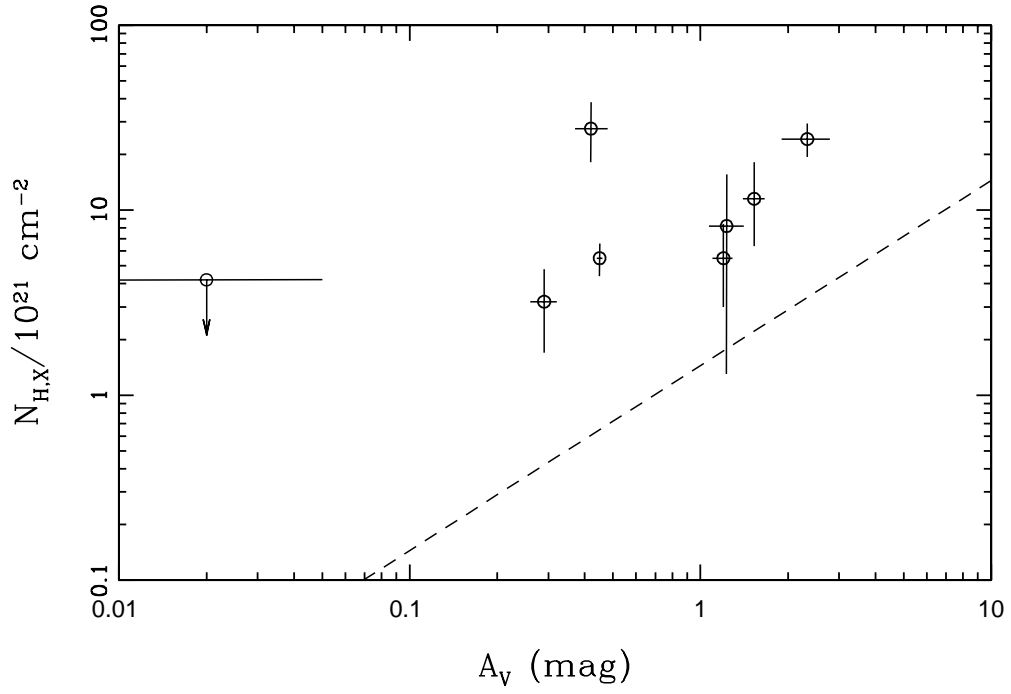


Fig. 2.— X-ray column density  $N_{\text{H,X}}$  plotted against dust extinction  $A_V$ . The dashed line shows the typical value of dust-to-gas ratio for the environment of the Local Group.

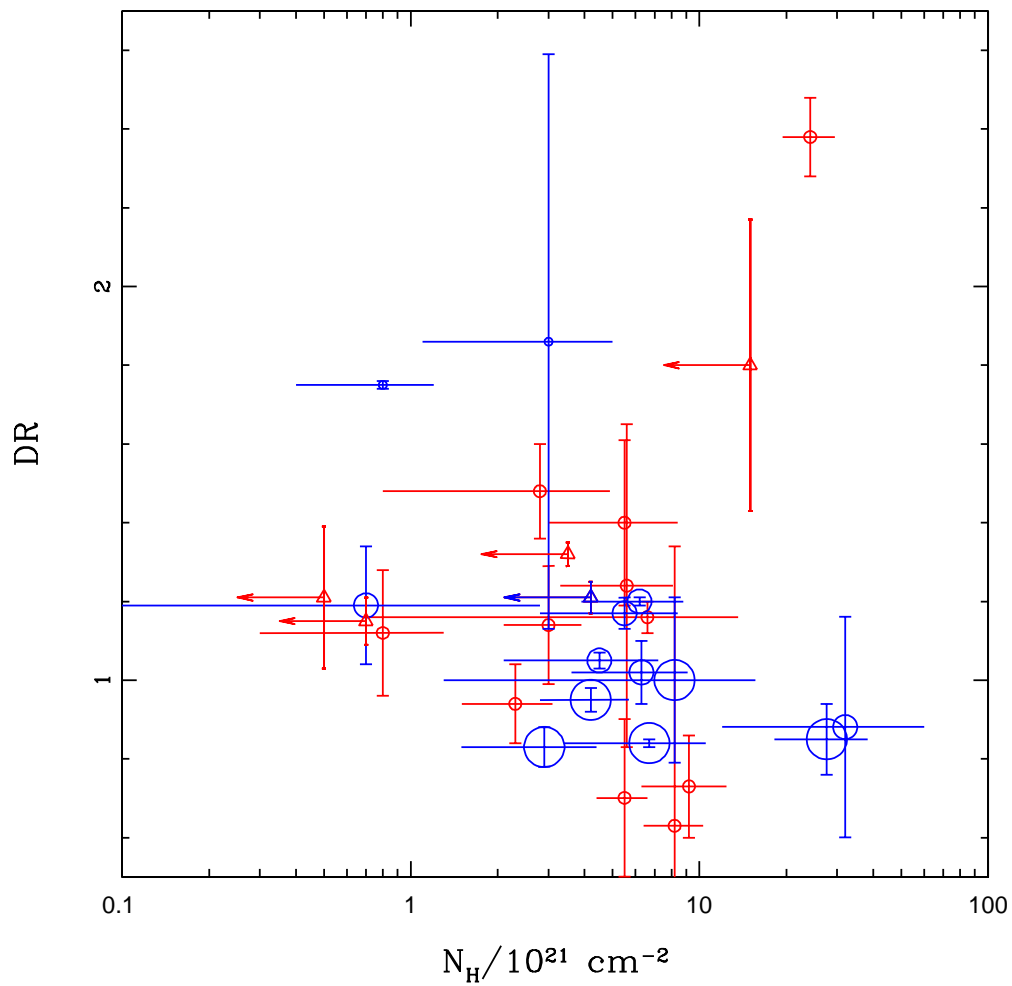


Fig. 3.— Relation between X-ray column density  $N_{H,X}$  and intervening Mg II DR for the bursts listed in our sample. The GRBs with the only upper limit of  $N_{H,X}$  are marked by the open triangles and arrows. The red and blue points show the lines-of-sight with single and multiple intervening absorption systems, respectively. The size of the blue points is scaled to the number of saturated absorbers with  $DR < 1.2$ . The errorbars correspond to the  $1\sigma$  significance level.

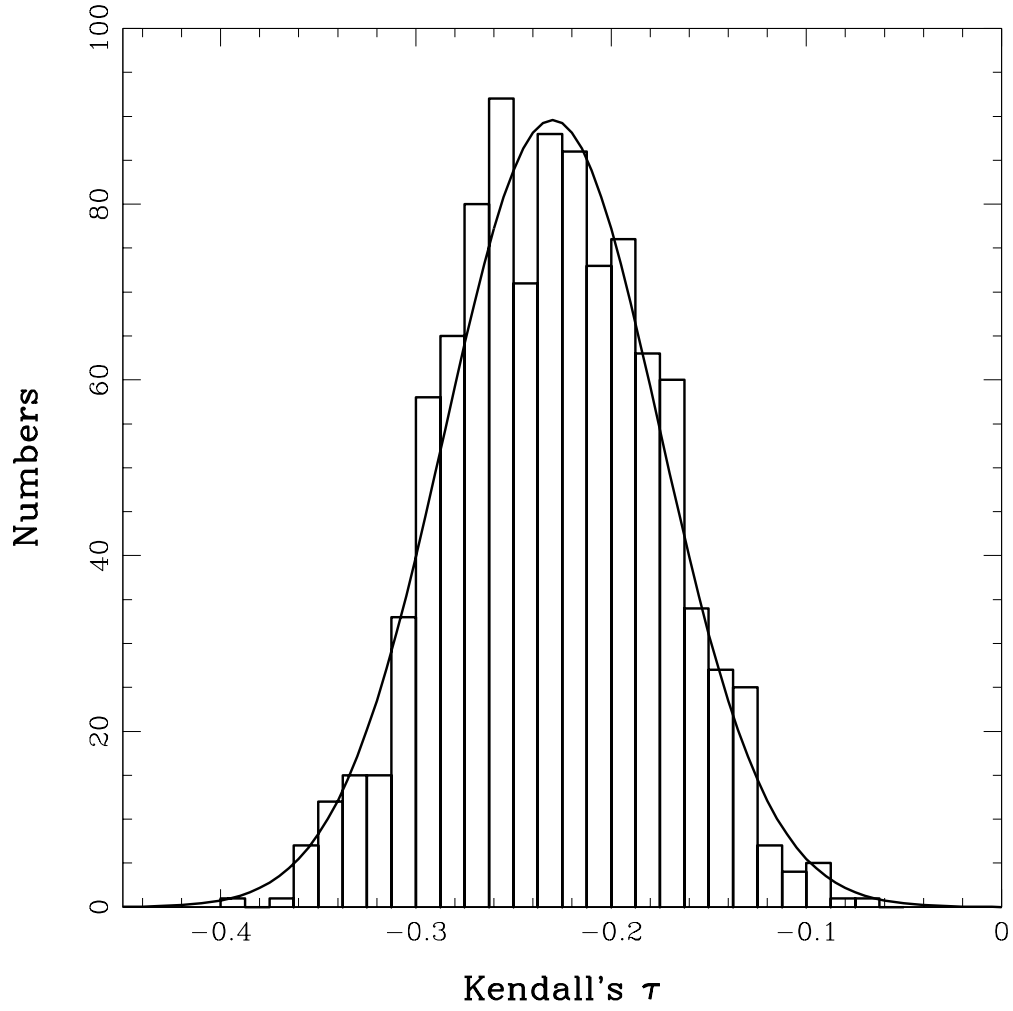


Fig. 4.— Distribution of the simulated Kendall's  $\tau$ . The best fit Gaussian function is shown by the solid line.

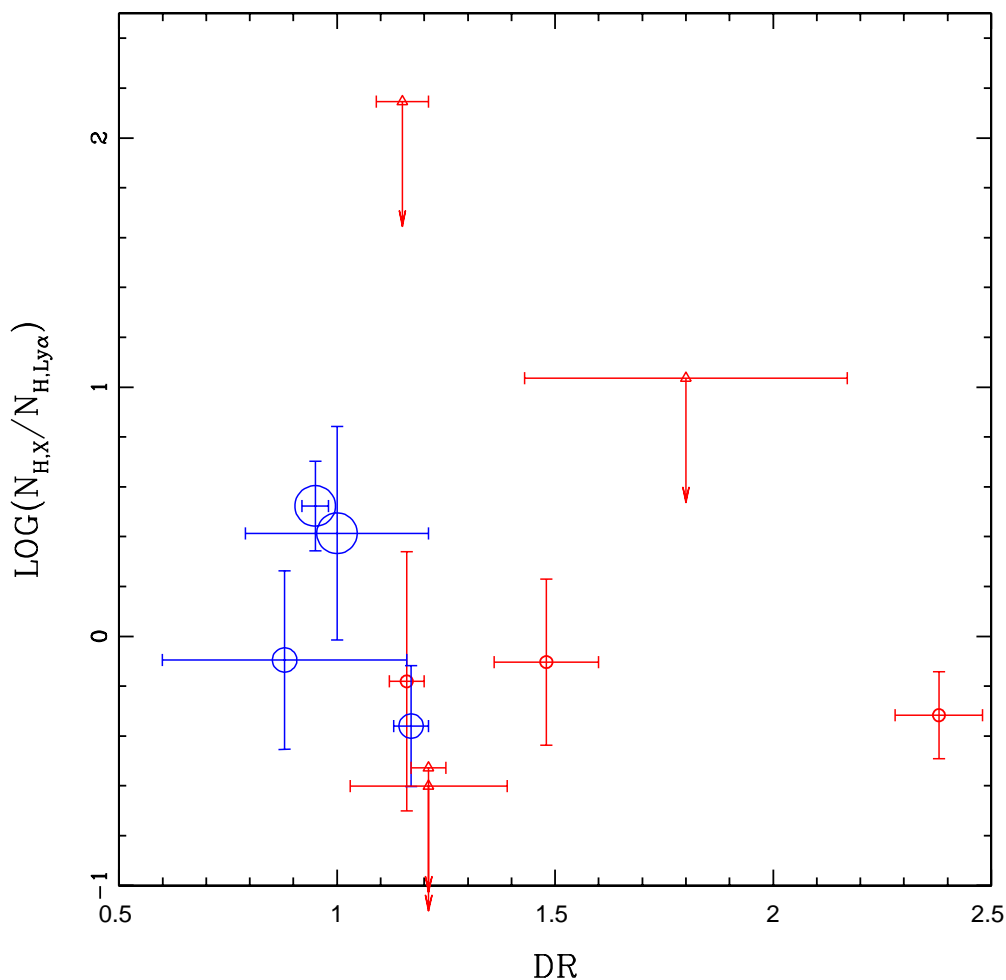


Fig. 5.— Mg II DR versus the ratio between  $N_{\text{H}}$  measured from the X-ray spectrum and that measured from local Lyman- $\alpha$  absorption. Again, the GRBs with only upper limits of  $N_{\text{H,X}}$  are marked by the open triangles and arrows. Two GRBs, GRB 060607 and GRB 050908, are not shown in the diagram because of their extremely large column density ratios (see text for details). The red and blue points show the lines-of-sight with single and multiple intervening absorption systems, respectively. The size of the blue points is scaled to the number of saturated absorbers with  $\text{DR} < 1.2$ . The errorbars correspond to the  $1\sigma$  significance level.

Table 1: Sample of *Swift* GRBs with detection of intervening Mg II doublet absorption.

GRB	$z_{\text{GRB}}$	$z_{\text{abs}}$	EW(2796) Å	DR	$N_{\text{H,X}}$ $10^{21} \text{ cm}^{-2}$	$N_{\text{HI}}$ $10^{21} \text{ cm}^{-2}$	$A_V$ mag	Reference
(1)	(2)	(3)	(4)	(5)	(6)	(7)	(8)	(9)
050730	3.97	<b>1.77317*</b> , 2.25378	$0.923 \pm 0.019$	$1.17 \pm 0.04$	$5.5^{+2.9}_{-2.7}$	$12.59 \pm 2.90$	.....	1,5
050820	2.6147	0.6915, <b>1.4288*</b> , 1.6204, 2.3598*	$1.203 \pm 0.023$	$0.95 \pm 0.03$	$4.2^{+1.5}_{-1.4}$	$1.26 \pm 0.29$	.....	2,5
050908	3.339	1.548	$1.21 \pm 0.02$	$1.32 \pm 0.03$	$< 3.5$	$(4, 0 \pm 0.9) \times 10^{-4}$	.....	2,5
050922C	2.199	1.10731	$0.532 \pm 0.031$	$1.48 \pm 0.12$	$2.8^{+2.1}_{-2.0}$	$3.55 \pm 0.82$	.....	1,5
051111	1.549	0.82735, <b>1.18910</b>	$2.091 \pm 0.011$	$1.20 \pm 0.01$	$6.2^{+2.6}_{-2.3}$	.....	.....	1
060418	1.49	<b>0.60259*</b> , 0.65593, 1.10724, 1.32221	$1.299 \pm 0.015$	$1.05 \pm 0.02$	$4.5^{+2.7}_{-2.4}$	.....	.....	1
060502A	1.515	1.044*, 1.078, <b>1.147*</b>	$2.39 \pm 0.12$	$0.83 \pm 0.05$	$2.9^{+1.5}_{-1.4}$	.....	.....	2
060607	3.082	1.51057, 1.80208, <b>2.2784*</b>	$0.293 \pm 0.015$	$1.02 \pm 0.08$	$6.3^{+2.8}_{-2.7}$	$(8.9 \pm 0.6) \times 10^{-5}$	.....	1,5
060926	3.2	<b>1.7954*</b> , 1.8289	$3.27 \pm 0.69$	$0.88 \pm 0.28$	$32.0^{+28.0}_{-20.0}$	$39.8 \pm 13.8$	.....	2,5
061007	1.261	1.065	$3.14 \pm 0.53$	$0.70 \pm 0.20$	$5.5^{+1.1}_{-1.1}$	.....	$0.45^{+0.01}_{-0.01}$	2,6
070506	2.306	1.6	$1.92 \pm 0.04$	$1.16 \pm 0.04$	$6.6^{+7.0}_{-5.9}$	$10.0 \pm 6.9$	.....	2,5
070611	2.039	1.297	$2.65 \pm 0.27$	$1.21 \pm 0.18$	$< 0.5$	$3.2 \pm 1.5$	.....	2,5
070802	2.45	<b>2.0785*</b> , 2.2921*	$0.82 \pm 0.12$	$1.00 \pm 0.21$	$8.2^{+7.4}_{-6.9}$	$21.50 \pm 0.20$	$1.23^{+0.18}_{-0.16}$	2,5,7
071003	1.604	<b>0.372*</b> , 0.943, 1.101	$2.28 \pm 0.19$	$1.19 \pm 0.15$	$0.7^{+2.1}_{-0.6}$	.....	.....	2
071031	2.6922	1.0743, 1.6419, <b>1.9520</b>	$0.743 \pm 0.016$	$1.21 \pm 0.04$	$< 4.2$	$14.1 \pm 1.6$	$0.02^{+0.03}_{-0.02}$	2,5,7
080310	2.4272	1.6711	$0.421 \pm 0.012$	$1.15 \pm 0.06$	$< 0.7$	.....	.....	2
080319B	0.94	<b>0.5308</b> , 0.5662, 0.7154, 0.7608	$0.614 \pm 0.001$	$1.75 \pm 0.01$	$0.8^{+0.4}_{-0.4}$	.....	.....	2
080319C	1.95	0.8104	$2.04 \pm 0.52$	$1.24 \pm 0.41$	$5.6^{+2.5}_{-2.3}$	.....	.....	2
080603A	1.688	1.271*, <b>1.563*</b>	$0.77 \pm 0.01$	$0.84 \pm 0.01$	$6.7^{+3.8}_{-3.3}$	.....	.....	2
080605	1.64	1.2987	$1.08 \pm 0.11$	$1.40 \pm 0.21$	$5.5^{+2.9}_{-2.5}$	.....	$1.2^{+0.1}_{-0.1}$	2
080607A	3.036	1.341	$3.0 \pm 0.08$	$2.38 \pm 0.10$	$24.2^{+5.2}_{-4.8}$	$50.1 \pm 17.3$	$2.33^{+0.46}_{-0.43}$	2,5,8
081222	2.77	<b>0.8168</b> , 1.0708	$0.52 \pm 0.01$	$1.86 \pm 0.73$	$3.0^{+2.0}_{-1.9}$	.....	.....	2
090313	3.37	1.80*, <b>1.96*</b>	$0.50 \pm 0.03$	$0.85 \pm 0.09$	$27.6^{+10.7}_{-9.4}$	.....	$0.42^{+0.06}_{-0.05}$	3,7
091208B	1.063	0.784	$0.65 \pm 0.43$	$0.63 \pm 0.71$	$8.2^{+2.1}_{-1.8}$	.....	.....	2
100219A	4.6667	2.18	$0.90 \pm 0.08$	$1.80 \pm 0.37$	$< 15.0$	$1.38 \pm 0.16$	.....	4,5
100814A	1.44	1.1574	$0.426 \pm 0.04$	$1.12 \pm 0.16$	$0.8^{+0.5}_{-0.5}$	.....	.....	2
100901A	1.408	1.314	$1.74 \pm 0.17$	$1.14 \pm 0.15$	$3.0^{+0.9}_{-0.9}$	.....	.....	2
100906A	1.64	0.994	$0.87 \pm 0.10$	$0.73 \pm 0.13$	$9.2^{+3.2}_{-2.9}$	.....	.....	2
110918A	0.982	0.877	$2.65 \pm 0.20$	$0.94 \pm 0.10$	$2.3^{+0.8}_{-0.8}$	.....	.....	2

Note. — References in the last column: 1-Tejos et al. (2009); 2-Cucchiara et al. (2012); 3-de Ugarte Posigo et al. (2010); 4-Thone et al. (2013); 5-Fynbo et al. (2009); 6-Schady et al. (2010); 7-Greiner et al. (2011); 8-Zafar et al. (2011)